

## Expected Variations of Small-scale Cosmic Ray Anisotropies with Time and Energy

Wenyi Bian<sup>a,b,\*</sup> and Gwenael Giacinti<sup>a,b</sup>

<sup>a</sup>*Tsung-Dao Lee Institute, Shanghai Jiao Tong University,  
520 Shengrong Road, Shanghai 201210, P. R. China*

<sup>b</sup>*School of Physics and Astronomy, Shanghai Jiao Tong University,  
800 Dongchuan Road, Shanghai 201210, P. R. China*

*E-mail:* [bianwenyi@sjtu.edu.cn](mailto:bianwenyi@sjtu.edu.cn), [gwenael.giacinti@sjtu.edu.cn](mailto:gwenael.giacinti@sjtu.edu.cn)

The arrival directions of TeV cosmic rays on the sky display an anisotropy at the 0.1 percent level. This anisotropy contains a dipole and higher order multipoles. Small-scale anisotropies should contain important information about the properties of the turbulent magnetic fields in the interstellar medium [1]. These anisotropies have been predicted to vary on a time-scale of a decade at TeV energies [2]. To date, no time variation has been detected. Whether experiments can detect such time variations or not depends on their energy resolutions ( $\Delta E/E$ ). Finite energy resolutions can result in substantial changes of the anisotropy at small scales. Compared to previous works on this topic, we consider here the effect of the energy resolution on the detectability of time variations. We use the code of this work [1]. We find that the amplitude of the difference between two instants in time will be smaller than in calculations where the energy resolution is not taken into account. We also study in detail the energy dependence of the small-scale anisotropies. We find that the amplitudes of the observed small-scale anisotropy structures are larger with a better energy resolution.

38th International Cosmic Ray Conference (ICRC2023)  
26 July - 3 August, 2023  
Nagoya, Japan



---

\*Speaker

## 1. Introduction

The transport of Cosmic Rays(CRs) in the our galaxy is usually approximated as a diffusive process. The Cosmic Rays propagate in our Galaxy for millions year before we measure them on the Earth, so they come almost isotropically from all direction of the sky. However experiments measure a small anisotropy in the Cosmic Rays flux observed at the Earth. The amplitude of this anisotropy is about  $10^{-3}$ . The dipole anisotropy is thought to be related to the density gradient of CRs near the solar system, and can be described by the following equation  $\vec{\delta} \simeq (3D/c)(\vec{\nabla}n/n)$  where  $D$  is diffusion coefficient and  $n$  is density of CRs. The higher order multipoles (quadrupole, octupole and so on), corresponding to the small-scale anisotropy structures, are suggested to be caused by the turbulent magnetic field in the interstellar medium(ISM) [1][3].

This work[2] has suggested that if the CR anisotropy at small angular scales is mainly due to the local turbulence, then small-scale anisotropies should be variable on the time-scale corresponding to the traveling distance of the Earth which is equal to CR gyroradius.

So far, this time variation of this cosmic ray sky-map has not been detected in experimental observations yet. One possible reason we suggest in the present work is that the finite energy resolution can have an impact on the detectability of the time variations. The anisotropy structures are also highly depending in the CR energies. If the detector's actual energy resolution is relatively low, it can lead to differences between the observed anisotropy structures and the theoretically expected anisotropy structures.

## 2. Simulation Method

In our simulation, we use the "Grid Method" to store the magnetic field in which we propagate our test CR particles. The standard grid method is storing the turbulent magnetic fields in spatial grid points[4]. We generate the turbulent magnetic field by the "Nested grid method" which is described in this work[5]. The set of parameters for the three repeated cubes in our simulation is presented in Table 1. The turbulent magnetic field we use here is Kolmogorov turbulence, and we propagate test CR particles separately. The motion is calculated by integrating the Lorentz force.

**Table 1:** Main parameters in simulations.

$N_{step}$	$L_{min}$	$L_{max}$	$l_c$	$\bar{B}$
256	2.5 pc	150 pc	$\sim 30$ pc	$4 \mu G$

## 3. CR anisotropy variation with energy

In the first section, we have already noted that experiments have detected the energy-dependent anisotropy of CR. In this section, we give our simulated results from 1 PeV energy to 100 PeV energy. In Figure 1, we present our simulation results for one given observer location at 4 different energies. It is obvious that the anisotropy structures show differences at these energy bins on both their multipole phases and amplitudes.

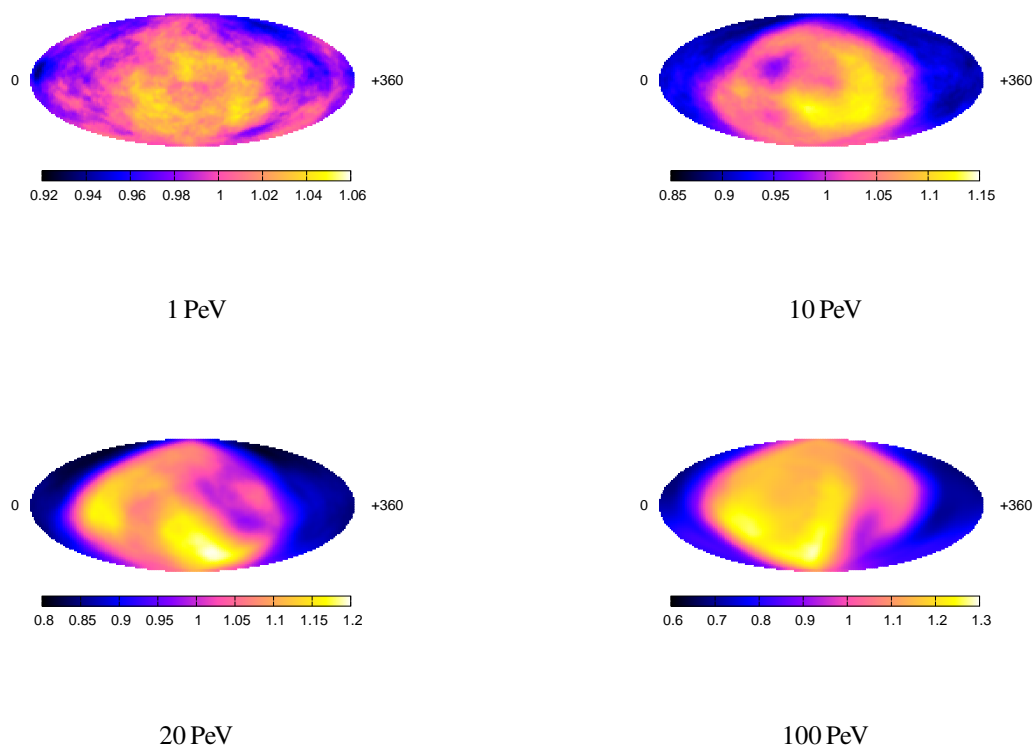


**Figure 1:** Anisotropies of the CR intensity at the same location with different energies. The anisotropy structures are clearly different at different energies.

In Figure 2, we make the "difference map" to describe the differences between anisotropies at two different energies, or two different locations. "Difference maps" show, at each point on the sky, the difference between the CR intensity in the two sky maps. The maximum value of the "difference map" is already equal to the anisotropy amplitude in this case, which means that the anisotropies have already changed substantially with energy varying from 10 PeV to 20 PeV.

In Figure 3, we present the simulated results taking into account the detector energy resolution. Here, we model the energy resolution by using CRs with an energy distribution that follows a Gaussian distribution in logarithmic space of energy. The resolution we set here is  $\Delta E/E = 0.4$  and we set the  $E_{min}$  and  $E_{max}$  as 1 and 100 PeV. The mixed energy anisotropy structure compared with the result for fixed energy shows obvious differences. The structures, especially the small-scale ones are somehow hidden by the finite energy resolution.

#### 4. Time Variations of Anisotropies

In Figure 4, we present simulation results for cosmic rays with 20 PeV CR energy located at different observing positions. As the distance of the observer's position changes and approaches the gyroradius of CR particles, the amplitude of the difference skymaps becomes increasingly closer to the magnitude of the anisotropy. This is in line with the findings of the work[2]. This means the

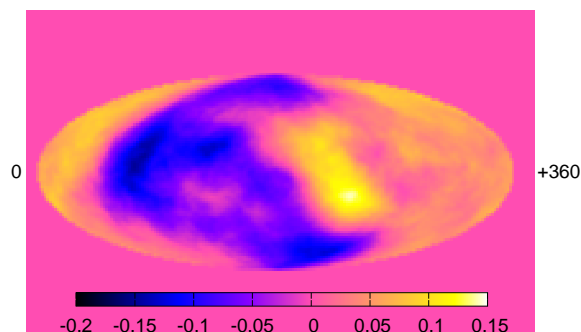
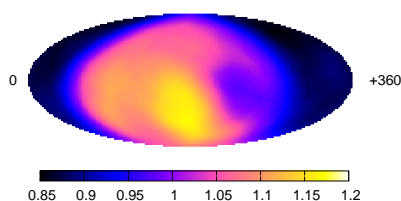
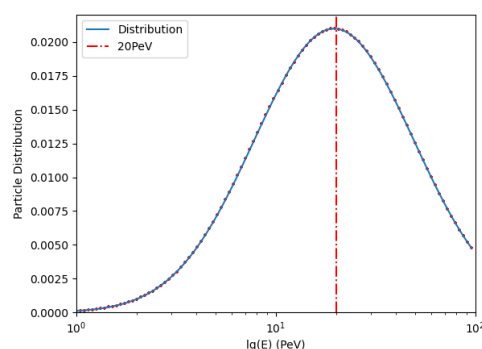


**Figure 2:** Map of the difference between the CR intensity maps at 10 PeV and 20 PeV. In this shown example, we subtract the values of 20 PeV map from the values of 10 PeV map.



20 PeV,  $\sigma = 0.4$ , Anisotropy



Energy distribution of CR particles

**Figure 3:** The left panel is the simulation result of the anisotropy at 20 PeV peak energy with a given energy resolution,  $\sigma = 0.4$ . The right distribution is the particle energy distribution used in the simulation.

variation of small-scale anisotropy structures becomes obvious after traveling  $r_g$  which is 5 pc in this case.

In Figure 5, after considering the effect of detector energy resolution, the time variations of anisotropies are clearly weaker than for the single energy results. After traveling around a 5 times bigger distance than  $r_g$  at 20 PeV which is the peak energy of the given distribution, the variation of small-scale anisotropy start to get close to the initial anisotropy amplitude level. This could be the reason why no experiment has detected the time variation of small-scale CR anisotropy. In Figure 6, we give the difference amplitude plots for different energy resolutions. As the  $\sigma$  increase, the change of small-scale anisotropy structures becomes more and more slow.

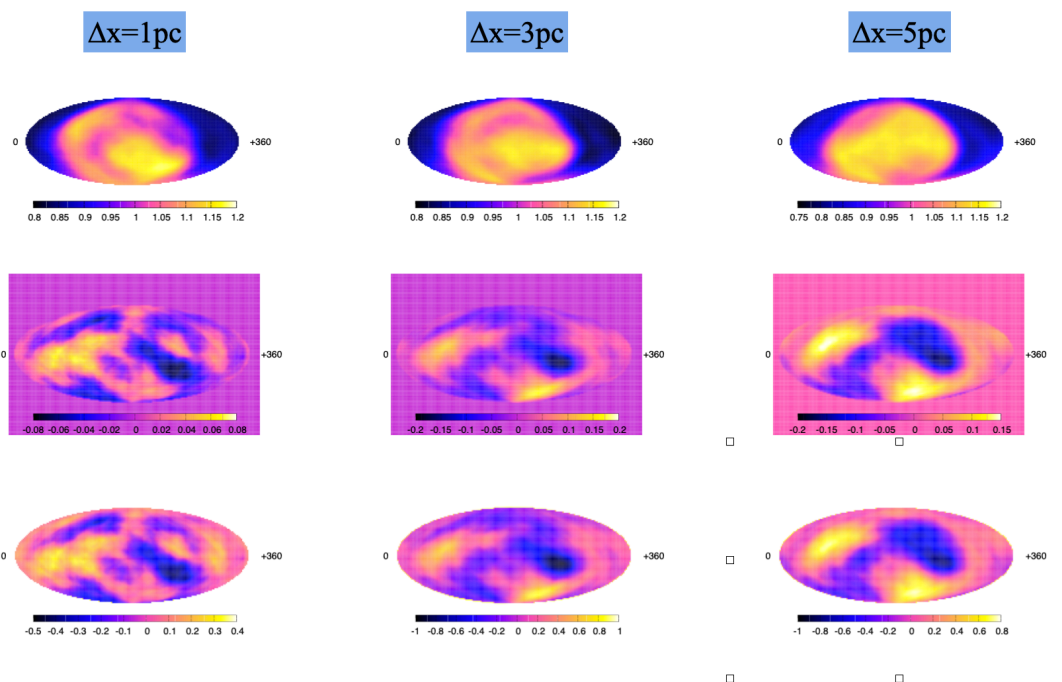


**Figure 4:**  $\Delta x$  represents the traveling distance between the two observer locations. The first row of the images shows the intensity sky-maps of cosmic rays at different positions, while the second row displays the difference sky-maps at each position compared with the initial position. The third row of the images represents the re-normalized difference skymaps, which represent the proportion of the amplitude of the anisotropy in the skymaps at each point compared to the initial skymap.

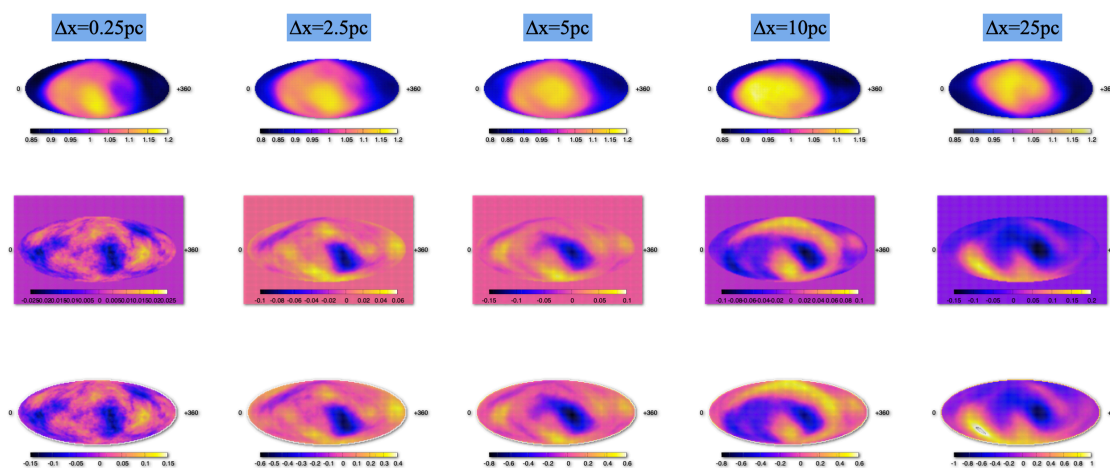


**Figure 5:** Energy distribution with 20 PeV peak energy and  $\sigma = 0.4$ . Each row in the figure is same as in Figure 4, but instead of representing results for a single energy, it shows the difference skymaps considering the energy resolution.

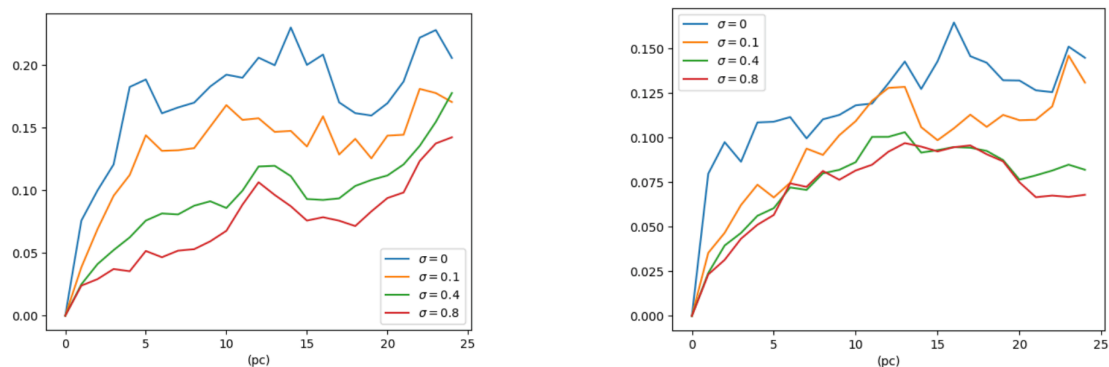


**Figure 6:** The maximum amplitude of difference sky-maps at different traveling distances of observer are presented in this figure. The two panels are for two different initial observer locations.

## 5. Conclusion

In this work, we discussed the impact of detector energy resolution on the temporal variations of anisotropy which has never been considered before. We find that the finite energy resolution has a significant impact on the detectability of the temporal variations, which could be a possible reason why such differences have not been detected experimentally so far.

**References**

- [1] G. Giacinti and G. Sigl, *Local magnetic turbulence and tev–pev cosmic ray anisotropies*, *Physical Review Letters* **109** (2012) 071101.
- [2] R. Kumar, N. Globus, D. Eichler and M. Pohl, *Time variability of tev cosmic ray sky map*, *Monthly Notices of the Royal Astronomical Society* **483** (2019) 896.
- [3] M. Ahlers and P. Mertsch, *Small-scale anisotropies of cosmic rays from relative diffusion*, *The Astrophysical Journal Letters* **815** (2015) L2.
- [4] P. Mertsch, *Test particle simulations of cosmic rays*, *Astrophysics and Space Science* **365** (2020) 135.
- [5] G. Giacinti, M. Kachelrieß, D. Semikoz and G. Sigl, *Cosmic ray anisotropy as signature for the transition from galactic to extragalactic cosmic rays*, *Journal of Cosmology and Astroparticle Physics* **2012** (2012) 031.